Encyclopedia of emergent particles in type-IV magnetic space groups

Zeying Zhang,[1,*] Gui-Bin Liu,[2,3,*] Zhi-Ming Yu,[2,3] Shengyuan A. Yang,[4] and Yugui Yao[2,3,†]

[1]*College of Mathematics and Physics, Beijing University of Chemical Technology, Beijing 100029, China*

[2]*Centre for Quantum Physics, Key Laboratory of Advanced Optoelectronic Quantum Architecture and Measurement (MOE), School of Physics, Beijing Institute of Technology, Beijing 100081, China*

[3]*Beijing Key Lab of Nanophotonics & Ultrafine Optoelectronic Systems, School of Physics, Beijing Institute of Technology, Beijing 100081, China*

[4]*Research Laboratory for Quantum Materials, Singapore University of Technology and Design, Singapore 487372, Singapore*

(Received 30 December 2021; accepted 2 March 2022; published 25 March 2022)

The research on emergent particles in condensed matters has been attracting tremendous interest, and recently it is extended to magnetic systems. Here, we study the emergent particles stabilized by the symmetries of type-IV magnetic space groups (MSGs) based on our classification of emergent particles in 230 gray space groups [Yu *et al.*, Sci. Bull. **67**, 375 (2022)]. Type-IV MSGs feature a special time reversal symmetry $\{\mathcal{T}|\boldsymbol{t}_0\}$, namely, the time reversal operation followed by a half lattice translation, which significantly alters the symmetry conditions for stabilizing the band degeneracies. In this work, based on symmetry analysis and modeling, we present a complete classification of emergent particles in type-IV MSGs by studying all possible (spinless and spinful, essential and accidental) particles in each of the 517 type-IV MSGs. Particularly, the detailed correspondence between the emergent particles and the type-IV MSGs that can host them are given in easily accessed interactive tables, where the basic information of the emergent particles, including the symmetry conditions, the effective Hamiltonian, the band dispersion, and the topological characters, can be found. According to the established encyclopedia, we find that several emergent particles that are previously believed to exist only in spinless systems will occur in spinful systems here, and vice versa, due to the $\{\mathcal{T}|\boldsymbol{t}_0\}$ symmetry. Our work not only deepens the understanding of the symmetry conditions for realizing emergent particles but also provides specific guidance for searching and designing materials with target particles.

DOI: 10.1103/PhysRevB.105.104426

I. INTRODUCTION

In crystals, the atoms are arranged in an orderly manner, forming crystal lattices extending in three directions in real space and leading to periodic band structure in momentum space [1]. The symmetries of the bare crystal lattice are described by the space groups, where all the operators can be made unitary. By further including the spin and orbital degrees of freedom in the crystal, antiunitary operations such as time reversal and its combinations with certain spatial symmetries need to be considered, and the extension leads to the magnetic space groups. Correspondingly, the energy bands of crystals should be labeled by the corepresentation of the relevant MSG [2–4].

With certain symmetry conditions, the energy bands may form degeneracies in the Brillouin zone (BZ), giving rise to topological semimetal states [5–17]. Because the degeneracies are singularities in momentum space, the excitations around the degeneracies show many novel and intriguing phenomena, such as chiral anomaly, quantum vortex, chiral Landau levels, and divergent optical responses [17–27]. Hence the topological semimetals have been one of the most active research fields in the past 10 years [28–33].

Rooted in the MSG symmetries and the corepresentations, the band degeneracies take diverse forms and each kind of degeneracy can exhibit distinct properties [34–45]. Thus it is of fundamental importance to list and classify all possible band degeneracies, along with their symmetry conditions. A complete classification of emergent particles in type-II and type-III MSGs have recently been presented by us in Ref. [46] and Ref. [47], respectively. Here, we complete the last missing piece of the project, i.e., the classification for the type-IV MSGs.

There are 517 type-IV MSGs, which share the following structure:

$$\mathbf{M} = \mathbf{G} + \{\mathcal{T}|\boldsymbol{t}_0\}\mathbf{G}, \tag{1}$$

where $\mathbf{G}$ is a space group, $\mathcal{T}$ is the time reversal operation, and $\boldsymbol{t}_0$ is a half lattice translation. The "shifted" time reversal operation $\{\mathcal{T}|\boldsymbol{t}_0\}$ connects two lattice sites with opposite magnetic moments, indicating that type-IV MSGs describe systems with certain antiferromagnetic orders. The appearance of $\{\mathcal{T}|\boldsymbol{t}_0\}$ is also reminiscent of nonsymmorphic symmetries, which are point group operations followed by a fractional lattice translation. Because of $\{\mathcal{T}|\boldsymbol{t}_0\}$, although the crystals belonging to type-IV MSG are magnetic systems without the pure $\mathcal{T}$ symmetry, its energy band still exhibits the $\mathcal{T}$

*These authors contributed equally to this work.
†ygyao@bit.edu.cn

TABLE I. Main results of the difference between type-IV magnetic space group and type-II MSG. "√" ("×") means there (do not) exist corresponding emergent particles in magnetic space groups. "II" and "IV" represent the type-II MSG and type-IV magnetic space group, respectively. The "√" with red color means that the emergent particles exist in type-IV magnetic space group but do not exist in type-II MSG, and the "√" with green color means that the emergent particles exist in type-II MSG but do not exist in type-IV magnetic space group. "Single (Double)" is for emergent particles with (without) SOC.

		Single		Double				Single		Double	
Notation	Abbr.	II	IV	II	IV	Notation	Abbr.	II	IV	II	IV
Charge-1 Weyl point	C-1 WP	√	√	√	√	Charge-2 Weyl point	C-2 WP	√	√	√	√
Charge-3 Weyl point	C-3 WP	√	√	√	√	Charge-4 Weyl point	C-4 WP	√	√	×	√
Triple point	TP	√	×	√	×	Charge-2 triple point	C-2 TP	√	√	√	√
Quadratic triple point	QTP	√	√	×	×	Quadratic contact triple point	QCTP	√	√	×	×
Dirac point	DP	√	√	√	√	Charge-2 Dirac point	C-2 DP	√	√	√	√
Charge-4 Dirac point	C-4 DP	×	√	√	√	Quadratic Dirac point	QDP	√	√	√	√
Charge-4 quadratic Dirac point	C-4 QDP	×	√	√	√	Quadratic contact Dirac point	QCDP	×	×	√	√
Cubic Dirac point	CDP	×	×	√	√	Cubic crossing Dirac point	CCDP	√	√	×	×
Sextuple point	SP	√	√	√	√	Charge-4 sextuple point	C-4 SP	×	√	√	×
Quadratic contact sextuple point	QCSP	×	×	√	×						
Octuple point	OP	×	×	√	√						
Weyl nodal line	WNL	√	√	√	√	Weyl nodal line (net)	WNLs	√	√	√	√
Quadratic nodal line	QNL	√	√	√	√	Cubic nodal line	CNL	×	×	√	√
Dirac nodal line	DNL	√	√	√	√	Dirac nodal line (net)	DNLs	√	√	√	√
Nodal surface	NS	√	√	√	√	Multiple nodal surfaces	NSs	√	√	√	√

symmetry, reflected as $E_n(\boldsymbol{k}) = E_n(\mathcal{T}\boldsymbol{k})$. However, the $\{\mathcal{T}|\boldsymbol{t}_0\}$ here is quiet different from the pure $\mathcal{T}$ symmetry but similar to the nonsymmorphic spatial operators. The extra fractional translation may lead to new possibilities of the emergent particles in type-IV MSGs. For example, consider the eight time-reversal invariant momenta (TRIMs) in the spinless case $\{\mathcal{T}|\boldsymbol{t}_0\}^2 = e^{-2i\boldsymbol{k}\cdot\boldsymbol{t}_0}$ will generate double degeneracy at TRIMs which satisfy $2\boldsymbol{k}\cdot\boldsymbol{t}_0 = \pi$. This is distinct from other space groups, where the pure $\mathcal{T}$ symmetry can lead to the Kramers double degeneracy only for spinful systems.

In this work, we systematically study all the possible emergent particles protected by the symmetries of type-IV MSGs and classify the emergent particles from four aspects, namely, the dimension of degeneracy manifold, the degree of degeneracy, the type of dispersion, and the topological charge. The main results are shown in Table I, where one can find most of the emergent particles (except QCSP) can be realized in type-IV MSGs. The corepresentation information and the possible emergent particles, including spinless and spinful, essential, and accidental particles for each of the 517 type-IV MSGs are given in easily accessible interactive tables in S6 of the Supplemental Material (SM) [48]. We also compare the differences between results of type-IV MSGs and that of type-II MSGs (nonmagnetic systems with pure $\mathcal{T}$ symmetry) in Table I. For type-II MSGs, the C-4 WP only appears in spinless systems while the C-4 DP, the C-4 QDP, and the C-4 SP only appear in spinful systems [46]. In contrast, for type-IV MSGs the C-4 SP only appear in spinless systems, and the C-4 WP, the C-4 DP, and the C-4 QDP can appear in both spinless and spinful systems, due to the $\{\mathcal{T}|\boldsymbol{t}_0\}$ symmetry. We construct concrete lattice models to demonstrate the existence of C-4 WP in spinful systems and the existence of C-4 DP in spinless systems. Together with Refs. [46] and [47], our work accomplishes the grand task of classifying all possible emergent particles in periodic lattices.

II. RATIONALE

To study the degeneracies stabilized by the symmetries of type-IV MSGs, we should obtain the corepresentation information of type-IV MSGs. The method to calculate the corepresentation information of type-IV MSGs are exactly the same as that of type-II MSGs [1]. Specifically, the corepresentation of a type-IV MSG $\mathbf{M}$ can be induced from the small corepresentations of $M_{\boldsymbol{k}}$, where $M_{\boldsymbol{k}}$ is the magnetic little group of $\boldsymbol{k}$ in $\mathbf{M}$. This step is done by our homemade package MSGCorep [49]. With the calculated small corepresentation information of $M_{\boldsymbol{k}}$, we can easily identify the possible degeneracies protected by the symmetries of $M_{\boldsymbol{k}}$ and establish the $\boldsymbol{k}\cdot\boldsymbol{p}$ Hamiltonians expanded around the corresponding degeneracy. Many crucial properties of the degeneracies can be inferred from the $\boldsymbol{k}\cdot\boldsymbol{p}$ Hamiltonians, such as the dimension of degeneracy manifold, the type of band splitting, and the topological charge. A complete list of all possible emergent particles and their detailed classification is presented in S5 of the SM, arranged for each of the 517 type-IV MSGs. We also list the correspondence between Belov-Nerenova-Smirnova (BNS) symbol [2,3] and Opechowski-Guccione (OG) symbol [4] for type-IV MSGs in S4 of the SM.

III. COMPARE WITH NONMAGNETIC SYSTEMS

We also compare the particles in type-IV MSGs with that in type-II MSGs (nonmagnetic systems), and the results are shown in Table I. All kinds of accidental band degeneracies on high symmetry lines found in type-II MSGs can also be realized in type-IV MSGs. Hence let us focus on the essential band degeneracies. First, a notable feature for type-IV MSGs is that the C-4 WP can exist in spinful systems. However, for nonmagnetic systems, the C-4 WP can only exist in spinless materials. Besides, the C-3 WP can appear as essential band

TABLE II. Complex emergent particles existing in type-IV MSGs. The format of this table is similar to Table I.

Notation	Abbr.	Single II	Single IV	Double II	Double IV	Notation	Abbr.	Single II	Single IV	Double II	Double IV
Combined WNL and NS	WNL/NS	√	√	√	√	Combined WNLs and NSs	WNLs/NSs	√	√	×	×
Combined QNL and NS	QNL/NS	×	√	×	√	Combined QNL and WNLs	QNL/WNLs	√	√	√	√
Combined QNLs and WNLs	QNLs/WNLs	√	×	×	×	Combined CNL and NS	CNL/NS	×	×	×	√
Combined CNL and WNLs	CNL/WNLs	×	×	×	√						

crossing protected by the single type-IV MSGs, but it is only allowed as accidental band crossing on a high symmetry line in type-II MSGs. Moreover, the C-4 DP, C-4 QDP, and C-4 SP emerged as spinful particles in nonmagnetic can exist in spinless systems belonging to type-IV MSGs.

Second, there are more possibilities of the complex particles in type-IV MSGs. Here the complex emergent particles refer to the degeneracies that include two or multiple different kinds of particles and these particles share one same degenerate point in BZ. For example, the complex particle CNL/NS in MSG 184.196 includes a CNL residing along ΓA line and a NS located at AHL plane, and the CNL and NS are connected at a joint point of A. However, such a CNL/NS complex particle cannot be realized in type-II MSGs. Besides, the complex particles of QNL/NS, CNL/NS, and CNL/WNLs can appear in type-IV MSGs but cannot occur at type-II MSGs, as shown in Table II.

IV. C-4 WP AND C-4 DP

According to previous results, the C-4 WP and C-4 DP only exist in spinless and spinful systems respectively for type-II MSGs. However, the $\{\mathcal{T}|\boldsymbol{t}_0\}$ symmetry brings new possibilities, making the realization of C-4 WP in spinful systems and that of C-4 DP in spinless systems. According to our classification (see S5-C of the SM), we find that the C-4 WP can be realized in the magnetic materials with SOC effect at the R point of MSG 198.11, 212.62, and 213.66. Here, we use a concrete spinful lattice model with MSG 198.11 to demonstrate the existence of C-4 WP. Part of the result in the SM for MSG 198.11 is shown in Table III. In this table, we present many important properties of MSG 198.11, including the information of the corresponding BZ, the corepresentation information of each high-symmetry momentum, and the possible degeneracies protected by the MSG symmetries.

There are four points which need to be clarified. (i) For the spinful cases with $I\mathcal{T}$ symmetry, all bands are at least doubly degenerate in the whole Brillouin zone due to the Kramers degeneracy $[(I\mathcal{T})^2 \equiv -1]$ and, for spinless cases with $I\mathcal{T}$, one can always choose the proper basis to obtain a real Hamiltonian; then the degeneracy manifold for the doubly degenerate point in those cases is always larger than zero, i.e., the degenerate point is on a nodal line or NS [12]. (ii) The blue text in S6 of the SM (marked as Greek letters and Latin capital letters) is clickable. One can directly click them to get the full form of corepresentation matrices and Hamiltonians. (iii) In order to avoid redundant data in S8 of the SM, the Hamiltonian marked as $H_n^{R_i}$ which means the expression of the Hamiltonian is exactly the same as the Hamiltonian in R_i corepresentation of magnetic space group n, despite the fact that their corepresentation matrices may differ. (iv) The symmetry operations for magnetic space groups are taken from Bradley and Cracknell's (BC) book [1]. However, some magnetic space groups are mistaken in the BC book, which are not consistent with their BNS notations [2,3]. These magnetic space groups are corrected in the package MSGCorep [49], and hence all magnetic space groups we used here are consistent with those used in Bilbao Crystallographic Server or ISOTROPY [50,51].

For the spinful systems with MSG 198.11, one has $\{\mathcal{T}|t_0\}^2 = -1$ for Γ, M and $\{\mathcal{T}|t_0\}^2 = 1$ for R, X, as $t_0 = (\frac{1}{2}\frac{1}{2}\frac{1}{2})$. Hence the band in Γ and M must at least be doubly degenerate, while R and X do not have such constraints. The generators of corepresentation matrices for R_5R_6 of the R point can be written as

$$\begin{aligned} &D\left(\left\{C_{2z}\middle|\frac{1}{2}0\frac{1}{2}\right\}\right) = -D\left(\left\{C_{2x}\middle|\frac{1}{2}\frac{1}{2}0\right\}\right) = \sigma_0, \\ &D(\{C_{3z}|000\}) = \gamma\sigma_{19} = -\frac{1}{2}\sigma_0 - i\frac{\sqrt{3}}{2}\sigma_3, \\ &D\left(\left\{\mathcal{T}\middle|\frac{1}{2}\frac{1}{2}\frac{1}{2}\right\}\right) = \sigma_1, \end{aligned} \tag{2}$$

where the definition of σ_i and γ can be found in S7 of the SM. Then the $\boldsymbol{k}\cdot\boldsymbol{p}$ Hamiltonian at the R point can be solved from the constraint equations

$$H(\boldsymbol{k}) = \begin{cases} D(Q)H(R^{-1}\boldsymbol{k})D^{-1}(Q) & \text{if } Q = \{R|\boldsymbol{t}\}, \\ D(Q)H^*(-R^{-1}\boldsymbol{k})D^{-1}(Q) & \text{if } Q = \{R\mathcal{T}|\boldsymbol{t}\}, \end{cases} \tag{3}$$

where $D(Q)$ is the corepresentation matrices for symmetry operation Q with rotation part R and translation part $\boldsymbol{t}$. The $\boldsymbol{k}\cdot\boldsymbol{p}$ Hamiltonian for R_5R_6 is [52]

$$\begin{aligned} H =& (c_1 + c_2k^2)\sigma_0 + c_5k_xk_yk_z\sigma_3 \\ &+ \left(c_3k_x^2 + c_4k_y^2 - c_3k_z^2 - c_4k_z^2\right)\sigma_1 \\ &+ \frac{\sqrt{3}}{3}\left(c_3k^2 - 3c_3k_y^2 - c_4k^2 + 3c_4k_x^2\right)\sigma_2, \end{aligned} \tag{4}$$

where $k^2 = k_x^2 + k_y^2 + k_z^2$. Such Hamiltonian hosts (223) leading order of the band splitting and is a C-4 WP [46]. Moreover, for nonmagnetic spinful systems, the C-2 TP cannot appear at the $\mathcal{T}$-invariant point. But, as shown in Table II, the C-2 TP can appear at the R point, which again demonstrates the fact that type-IV MSG can exhibit many intriguing phenomena that cannot be realized in nonmagnetic systems.

To further confirm our results, we construct both spinless and spinful lattice models for MSG 198.11. Notice the minimum Wyckoff position of 198.11 is $8a$; consider the $|\phi_s\rangle$ (spinless) and $\{|\phi_s\uparrow\rangle, |\phi_s\downarrow\rangle\}$ (spinful) for each atom in $8a$.

TABLE III. Part of the emergent particles in type-IV magnetic space group 198.11. The text above the double line of the table is the basic information of magnetic space group, including the symbol of magnetic space group, the Bravais lattice, the generators of the magnetic space group, whether the combination of inversion symmetry (I) and $\mathcal{T}$ exists, and whether SOC is considered. The column for $\boldsymbol{k}$ shows the name and coordinate of high-symmetry momenta [1]. The column for "Generators" is the rotation part for generators of the magnetic little group of $\boldsymbol{k}$. The column for "Corep" is the information of corepresentation of $\boldsymbol{k}$'s magnetic little group, including the label, dimension, and corepresentation matrices for generators. The last three columns are the $\boldsymbol{k}\cdot\boldsymbol{p}$ Hamiltonian, type of emergent particles, and topological charge, respectively.

198.11, P_I2_13 — Γ_c, $\{C_{2z}|\frac{1}{2}0\frac{1}{2}\}$, $\{C_{2x}|\frac{1}{2}\frac{1}{2}0\}$, $\{C_{31}^{+}|000\}$, $\{\mathcal{T}|\frac{1}{2}\frac{1}{2}\frac{1}{2}\}$, without $I\mathcal{T}$

$\boldsymbol{k}$			Corep			$\boldsymbol{k}\cdot\boldsymbol{p}$	Node	
Name	$\boldsymbol{k}$ info	Generators	Label	Dim	Matrices	Hamiltonian	type	$\lvert\mathcal{C}\rvert$
Spinless emergent particles								
Γ	000	$C_{2z}, C_{2x}, C_{31}^{+}, \mathcal{T}$	$\Gamma_2\Gamma_3$	2	$\sigma_0, \sigma_0, -\gamma\sigma_{19}, \sigma_1$	$H_{195.3}^{\Gamma_2\Gamma_3}$	C-4 WP	4
			Γ_4	3	$-A_{37}, A_{18}, A_9, A_0$	$H_{195.3}^{\Gamma_4}$	C-2 TP	2
X	$0\frac{1}{2}0$	$C_{2x}, C_{2y}, \mathcal{T}$	X_1	2	$-\sigma_1, \sigma_4, \sigma_4$	$H_{18.22}^{Y_1}$	C-1 WP	1
R	$\frac{1}{2}\frac{1}{2}\frac{1}{2}$	$C_{2z}, C_{2x}, C_{31}^{+}, \mathcal{T}$	R_1	2	$-i\sigma_3, i\sigma_1, -\delta\sigma_{25}, \sigma_4$	$H_{195.3}^{\Gamma_5}$	C-1 WP	1
			R_2R_3	4	$-i\Gamma_{50}, i\Gamma_{30}, \eta\Gamma_{92}, -\Gamma_{13}$	$H_{195.3}^{\Gamma_6\Gamma_7}$	C-4 DP	4
Spinful emergent particles								
Γ	000	$C_{2z}, C_{2x}, C_{31}^{+}, \mathcal{T}$	Γ_5	2	$-i\sigma_3, -i\sigma_1, \delta\sigma_{25}, \sigma_4$	$H_{195.3}^{\Gamma_5}$	C-1 WP	1
			$\Gamma_6\Gamma_7$	4	$-i\Gamma_{50}, -i\Gamma_{30}, -\eta\Gamma_{92}, -\Gamma_{13}$	$H_{195.3}^{\Gamma_6\Gamma_7}$	C-4 DP	4
M	$\frac{1}{2}\frac{1}{2}0$	$C_{2x}, C_{2y}, \mathcal{T}$	M_5	2	$\sigma_1, -i\sigma_4, \sigma_4$	$H_{18.22}^{Y_1}$	C-1 WP	1
R	$\frac{1}{2}\frac{1}{2}\frac{1}{2}$	$C_{2z}, C_{2x}, C_{31}^{+}, \mathcal{T}$	R_5R_6	2	$\sigma_0, -\sigma_0, \gamma\sigma_{19}, \sigma_1$	$H_{195.3}^{\Gamma_2\Gamma_3}$	C-4 WP	4
			R_7	3	$A_{18}, A_{37}, -A_{12}, A_0$	$H_{198.11}^{R_7}$	C-2 TP	2

Then we can construct two tight-binding models (see S2-A of the SM for Hamiltonian, parameters, and detail coreps of lattice models) [53]. The structure for an active atom of the lattice model is shown in Fig. 1. Moreover, for the spinful case there is another C-4 DP located at Γ as shown in Fig. 1(b). The calculated band structure of this two models are plotted in Figs. 1(c) and 1(d). The topological charge for emergent particles can be obtained by calculating the Wilson loops on a sphere enclosing the WP (DP)

$$W(\theta) = \oint d\boldsymbol{k}\, \langle\psi(\boldsymbol{k})|i\nabla|\psi(\boldsymbol{k})\rangle\,, \tag{5}$$

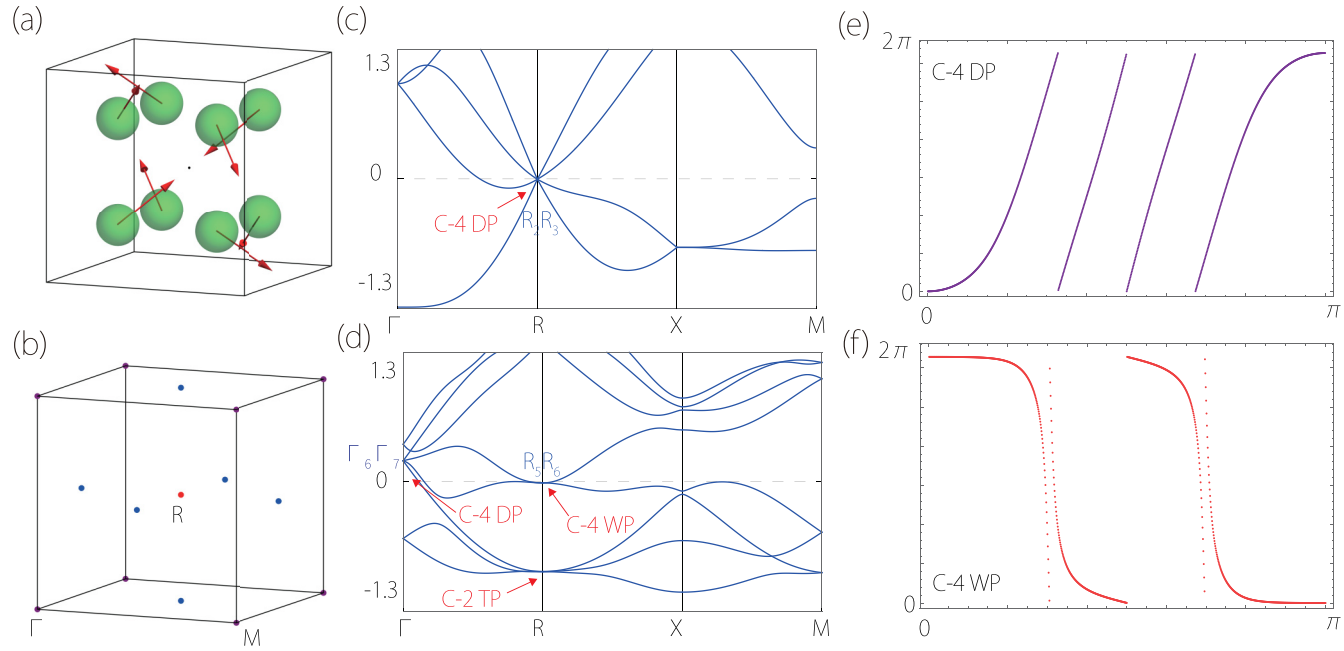

FIG. 1. (a) Structure of lattice model. (b) Schematic showing the C-4 WP, C-4 DP, and C-1 WPs in Brillouin zone; the red, purple, and blue points represent C-4 WP, C-4 DP, and C-1 WPs, respectively. (c),(d) Band structure of lattice models without SOC (c) and with SOC (d); the calculated coreps of the C-4 WP and C-4 DP are marked in blue. (e),(f) Wilson loop of C-4 DP and C-4 WP located at Γ (e) and R (f) and the horizontal coordinates are polar angle θ of the sphere.

where θ is the polar angle of the sphere. The integration is over an enclosing loop of a constant polar angle of the sphere. The calculated coreps of C-4 DP and C-4 WP [Figs. 1(c) and 1(d)] together with the evolution of the Wilson loop for Γ and R with considering SOC [Figs. 1(e) and 1(f)] are consist with Table III.

V. DISCUSSION AND CONCLUSION

In this work, we have theoretically listed the emergent particles in type-IV magnetic space groups. However, it remains an important task to identify realistic materials that can host these emergent particles. To put it into practice, one can directly look up our tables in S6 of the SM to find the possible emergent particles by the MSG number in the material database [54–56] (see S2-B of the SM for emergent particles in Nd_2CuO_4 as a real material example [57]). Besides, S5 of the SM also shows in which MSGs the specific emergent particles can exist. Experimentally, the spinful emergent particles can be directly probed by the angle-resolved photoemission spectroscopy (ARPES) method [58]. It can also break the $\mathcal{T}$ symmetry in artificial systems, which makes it possible to detect spinless emergent particles in type-IV MSGs, e.g., the $\mathcal{T}$ breaking photonic crystals can be realized by assembling magnetic rods [59,60]. The physical properties such as the magnetoresponse, transport behavior, topological surface states, and magneto-optical effect for emergent particles in a type-IV magnetic space group still need further investigation. For example, the large surface density of states for magnetic higher-order nodal lines might be beneficial for realizing surface magnetism and surface high-temperature superconductivity [41].

In conclusion, with the powerful tool of group representation theory, we establish the encyclopedia of emergent particles in type-IV magnetic space groups, which can provide useful guidance to search and study magnetic topological materials. Two interesting directions for the future are to (i) investigate the emergent particles in spin-space groups which have decoupled spin and lattice symmetries and (ii) use compatibility relations to study the connectivity of energy bands and the coexistence of emergent particles for specific Wyckoff position.

Note added. Recently, two independent and complementary works with a list of $\boldsymbol{k}\cdot\boldsymbol{p}$ Hamiltonians for 1651 magnetic space groups appeared in Refs. [61,62].

ACKNOWLEDGMENTS

This work is supported by the National Key R&D Program of China (Grant No. 2020YFA0308800), the NSF of China (Grants No. 12004028, No. 12004035, No. 11734003, No. 12061131002, and No. 52161135108), the China Postdoctoral Science Foundation (Grant No. 2020M670106), the Strategic Priority Research Program of Chinese Academy of Sciences (Grant No. XDB30000000), the Beijing Natural Science Foundation (Grant No. Z190006), and the Singapore MOE AcRF Tier 2 (Grant No. MOE2019-T2-1-001).

[1] C. Bradley and A. Cracknell, *Mathematical Theory of Symmetry in Solids: Representation Theory for Point Groups and Space Groups* (Oxford University Press, Oxford, 2009).
[2] N. V. Belov, N. N. Neronova, and T. S. Smirnova, 1651 Shubnikov groups, Sov. Phys. Crystallogr. **1**, 487 (1957).
[3] N. V. Belov, N. N. Neronova, and T. S. Smirnova, Shubnikov groups, Sov. Phys. Crystallogr. **2**, 311 (1957).
[4] W. Opechowski and R. Guccione, *Magnetic Symmetry* (Academic Press, New York, 1965).
[5] L. Michel and J. Zak, Connectivity of energy bands in crystals, Phys. Rev. B **59**, 5998 (1999).
[6] A. A. Burkov, M. D. Hook, and L. Balents, Topological nodal semimetals, Phys. Rev. B **84**, 235126 (2011).
[7] X. Wan, A. M. Turner, A. Vishwanath, and S. Y. Savrasov, Topological semimetal and Fermi-arc surface states in the electronic structure of pyrochlore iridates, Phys. Rev. B **83**, 205101 (2011).
[8] C. Fang, M. J. Gilbert, X. Dai, and B. A. Bernevig, Multi-Weyl Topological Semimetals Stabilized by Point Group Symmetry, Phys. Rev. Lett. **108**, 266802 (2012).
[9] B.-J. Yang and N. Nagaosa, Classification of stable three-dimensional Dirac semimetals with nontrivial topology, Nat. Commun. **5**, 5898 (2014).
[10] B. Q. Lv, H. M. Weng, B. B. Fu, X. P. Wang, H. Miao, J. Ma, P. Richard, X. C. Huang, L. X. Zhao, G. F. Chen, Z. Fang, X. Dai, T. Qian, and H. Ding, Experimental Discovery of Weyl Semimetal TaAs, Phys. Rev. X **5**, 031013 (2015).
[11] S. M. Young and C. L. Kane, Dirac Semimetals in Two Dimensions, Phys. Rev. Lett. **115**, 126803 (2015).
[12] H. Huang, J. Liu, D. Vanderbilt, and W. Duan, Topological nodal-line semimetals in alkaline-earth stannides, germanides, and silicides, Phys. Rev. B **93**, 201114(R) (2016).
[13] B. Bradlyn, J. Cano, Z. Wang, M. G. Vergniory, C. Felser, R. J. Cava, and B. A. Bernevig, Beyond Dirac and Weyl fermions: Unconventional quasiparticles in conventional crystals, Science **353**, aaf5037 (2016).
[14] T. Bzdušek, Q. Wu, A. Rüegg, M. Sigrist, and A. A. Soluyanov, Nodal-chain metals, Nature (London) **538**, 75 (2016).
[15] Z. Yan, R. Bi, H. Shen, L. Lu, S.-C. Zhang, and Z. Wang, Nodal-link semimetals, Phys. Rev. B **96**, 041103(R) (2017).
[16] W. Wu, Y. Liu, S. Li, C. Zhong, Z.-M. Yu, X.-L. Sheng, Y. X. Zhao, and S. A. Yang, Nodal surface semimetals: Theory and material realization, Phys. Rev. B **97**, 115125 (2018).
[17] Z.-M. Yu, W. Wu, X.-L. Sheng, Y. X. Zhao, and S. A. Yang, Quadratic and cubic nodal lines stabilized by crystalline symmetry, Phys. Rev. B **99**, 121106(R) (2019).
[18] A. A. Zyuzin and A. A. Burkov, Topological response in Weyl semimetals and the chiral anomaly, Phys. Rev. B **86**, 115133 (2012).
[19] A. A. Burkov, Chiral Anomaly and Diffusive Magnetotransport in Weyl Metals, Phys. Rev. Lett. **113**, 247203 (2014).
[20] X. Huang, L. Zhao, Y. Long, P. Wang, D. Chen, Z. Yang, H. Liang, M. Xue, H. Weng, Z. Fang, X. Dai, and G. Chen, Observation of the Chiral-Anomaly-Induced Negative Magne-

toresistance in 3D Weyl Semimetal TaAs, Phys. Rev. X **5**, 031023 (2015).
[21] T. Morimoto, S. Zhong, J. Orenstein, and J. E. Moore, Semiclassical theory of nonlinear magneto-optical responses with applications to topological Dirac/Weyl semimetals, Phys. Rev. B **94**, 245121 (2016).
[22] M. Hirschberger, S. Kushwaha, Z. Wang, Q. Gibson, S. Liang, C. Belvin, B. Bernevig, R. Cava, and N. Ong, The chiral anomaly and thermopower of Weyl fermions in the half-Heusler GdPtBi, Nat. Mater. **15**, 1161 (2016).
[23] T. Liu, M. Franz, and S. Fujimoto, Quantum oscillations and Dirac-Landau levels in Weyl superconductors, Phys. Rev. B **96**, 224518 (2017).
[24] J. E. Moore, Optical properties of Weyl semimetals, Natl. Sci. Rev. **6**, 206 (2019).
[25] Y. Okamura, S. Minami, Y. Kato, Y. Fujishiro, Y. Kaneko, J. Ikeda, J. Muramoto, R. Kaneko, K. Ueda, V. Kocsis, N. Kanazawa, Y. Taguchi, T. Koretsune, K. Fujiwara, A. Tsukazaki, R. Arita, Y. Tokura, and Y. Takahashi, Giant magneto-optical responses in magnetic Weyl semimetal $Co_3Sn_2S_2$, Nat. Commun. **11**, 4619 (2020).
[26] X. Yuan, C. Zhang, Y. Zhang, Z. Yan, T. Lyu, M. Zhang, Z. Li, C. Song, M. Zhao, P. Leng, M. Ozerov, X. Chen, N. Wang, Y. Shi, H. Yan, and F. Xiu, The discovery of dynamic chiral anomaly in a Weyl semimetal NbAs, Nat. Commun. **11**, 1259 (2020).
[27] Z. Song, J. Zhao, Z. Fang, and X. Dai, Detecting the chiral magnetic effect by lattice dynamics in Weyl semimetals, Phys. Rev. B **94**, 214306 (2016).
[28] M. Z. Hasan and C. L. Kane, Colloquium: Topological insulators, Rev. Mod. Phys. **82**, 3045 (2010).
[29] B. Bradlyn, L. Elcoro, J. Cano, M. G. Vergniory, Z. Wang, C. Felser, M. I. Aroyo, and B. A. Bernevig, Topological quantum chemistry, Nature (London) **547**, 298 (2017).
[30] N. P. Armitage, E. J. Mele, and A. Vishwanath, Weyl and Dirac semimetals in three-dimensional solids, Rev. Mod. Phys. **90**, 015001 (2018).
[31] C.-K. Chiu, J. C. Y. Teo, A. P. Schnyder, and S. Ryu, Classification of topological quantum matter with symmetries, Rev. Mod. Phys. **88**, 035005 (2016).
[32] H. C. Po, A. Vishwanath, and H. Watanabe, Symmetry-based indicators of band topology in the 230 space groups, Nat. Commun. **8**, 931 (2017).
[33] J. Yang, C. Fang, and Z.-X. Liu, Symmetry-protected nodal points and nodal lines in magnetic materials, Phys. Rev. B **103**, 245141 (2021).
[34] C. J. Bradley and B. L. Davies, Magnetic groups and their corepresentations, Rev. Mod. Phys. **40**, 359 (1968).
[35] R.-J. Slager, A. Mesaros, V. Jurii, and J. Zaanen, The space group classification of topological band-insulators, Nat. Phys. **9**, 98 (2013).
[36] R.-X. Zhang and C.-X. Liu, Topological magnetic crystalline insulators and corepresentation theory, Phys. Rev. B **91**, 115317 (2015).
[37] H. Watanabe, H. C. Po, and A. Vishwanath, Structure and topology of band structures in the 1651 magnetic space groups, Sci. Adv. **4**, eaat8685 (2018).
[38] J. Wang, Antiferromagnetic topological nodal line semimetals, Phys. Rev. B **96**, 081107(R) (2017).
[39] J. Kruthoff, J. de Boer, J. van Wezel, C. L. Kane, and R.-J. Slager, Topological Classification of Crystalline Insulators through Band Structure Combinatorics, Phys. Rev. X **7**, 041069 (2017).
[40] A. Bouhon, G. F. Lange, and R.-J. Slager, Topological correspondence between magnetic space group representations and subdimensions, Phys. Rev. B **103**, 245127 (2021).
[41] Z. Zhang, Z.-M. Yu, and S. A. Yang, Magnetic higher-order nodal lines, Phys. Rev. B **103**, 115112 (2021).
[42] L. Elcoro, B. J. Wieder, Z. Song, Y. Xu, B. Bradlyn, and B. A. Bernevig, Magnetic topological quantum chemistry, Nat. Commun. **12**, 5965 (2021).
[43] G. F. Lange, A. Bouhon, and R.-J. Slager, Subdimensional topologies, indicators, and higher order boundary effects, Phys. Rev. B **103**, 195145 (2021).
[44] T. He, X. Zhang, L. Wang, Y. Liu, X. Dai, L. Wang, and G. Liu, Ideal fully spin-polarized type-II nodal line state in half-metals X_2YZ_4, (X=K, Cs, Rb, Y=Cr, Cu, Z=Cl, F), Mater. Today Phys. **17**, 100360 (2021).
[45] W. Meng, X. Zhang, Y. Liu, X. Dai, and G. Liu, Antiferromagnetism caused by excess electrons and multiple topological electronic states in the electride $Ba_4Al_5 \cdot e^-$, Phys. Rev. B **104**, 195145 (2021).
[46] Z.-M. Yu, Z. Zhang, G.-B. Liu, W. Wu, X.-P. Li, R.-W. Zhang, S. A. Yang, and Y. Yao, Encyclopedia of emergent particles in three-dimensional crystals, Sci. Bull. **67**, 375 (2022).
[47] G.-B. Liu, Z. Zhang, Z.-M. Yu, S. A. Yang, and Y. Yao, Systematic investigation of emergent particles in type-III magnetic space groups, Phys. Rev. B **105**, 085117 (2022).
[48] See Supplemental Material at http://link.aps.org/supplemental/10.1103/PhysRevB.105.104426 for examples, correspondence between BNS symbol and OG symbol, elements of 517 MSGs, and detailed tables of the emergent particles in type-IV MSGs.
[49] G.-B. Liu *et al.*, MSGCorep: A package for corepresentations of magnetic space groups (unpublished).
[50] M. I. Aroyo, A. Kirov, C. Capillas, J. M. Perez-Mato, and H. Wondratschek, Bilbao Crystallographic Server. II. Representations of crystallographic point groups and space groups, Acta Crystallogr., A: Found. Crystallogr. **62**, 115 (2006).
[51] H. T. Stokes, D. M. Hatch, and B. J. Campbell, ISOTROPY Software Suite, https://iso.byu.edu/.
[52] Z. Zhang *et al.*, MagneticKP: A package for kp model of magnetic and non-magnetic materials (unpublished).
[53] Z. Zhang, Z.-M. Yu, G.-B. Liu, and Y. Yao, MagneticTB: A package for tight-binding model of magnetic and non-magnetic materials, Comput. Phys. Commun. **270**, 108153 (2022).
[54] S. Curtarolo, W. Setyawan, S. Wang, J. Xue, K. Yang, R. H. Taylor, L. J. Nelson, G. L. Hart, S. Sanvito, M. Buongiorno-Nardelli, N. Mingo, and O. Levy, AFLOWLIB.ORG: A distributed materials properties repository from high-throughput ab initio calculations, Comput. Mater. Sci. **58**, 227 (2012).
[55] S. V. Gallego, J. M. Perez-Mato, L. Elcoro, E. S. Tasci, R. M. Hanson, K. Momma, M. I. Aroyo, and G. Madariaga, *MAGNDATA*: towards a database of magnetic structures. I. The commensurate case, J. Appl. Crystallogr. **49**, 1750 (2016).
[56] A. Jain, S. P. Ong, G. Hautier, W. Chen, W. D. Richards, S. Dacek, S. Cholia, D. Gunter, D. Skinner, G. Ceder, and K. A. Persson, Commentary: The Materials Project: A materials

genome approach to accelerating materials innovation, APL Mater. **1**, 011002 (2013).

[57] S. Skanthakumar, J. W. Lynn, J. L. Peng, and Z. Y. Li, Observation of noncollinear magnetic structure for the Cu spins in Nd_2 CuO_4-type systems, Phys. Rev. B **47**, 6173 (1993).

[58] B. Lv, T. Qian, and H. Ding, Angle-resolved photoemission spectroscopy and its application to topological materials, Nat. Rev. Phys. **1**, 609 (2019).

[59] Z. Wang, Y. Chong, J. D. Joannopoulos, and M. Soljai, Observation of unidirectional backscattering-immune topological electromagnetic states, Nature (London) **461**, 772 (2009).

[60] L. Lu, C. Fang, L. Fu, S. G. Johnson, J. D. Joannopoulos, and M. Soljai, Symmetry-protected topological photonic crystal in three dimensions, Nat. Phys. **12**, 337 (2016).

[61] F. Tang and X. Wan, Exhaustive construction of effective models in 1651 magnetic space groups, Phys. Rev. B **104**, 085137 (2021).

[62] Y. Jiang, Z. Fang, and C. Fang, A $\boldsymbol{k}\cdot\boldsymbol{p}$ effective Hamiltonian generator, Chin. Phys. Lett. **38**, 077104 (2021).